

# IBIS: A Hybrid Inception-BiLSTM and SVM Ensemble for Robust Doppler-based Human Activity Recognition

Alison M. Fernandes, Hermes I. Del Monego, Bruno S. Chang, Anelise Munaretto, Helder Fontes and Rui Campos

**Abstract**—Wi-Fi sensing is a leading technology for Human Activity Recognition (HAR), offering a non-intrusive and cost-effective solution for healthcare and smart environments. Despite its potential, existing methods struggle with domain shift issues, often failing to generalize to unseen environments due to overfitting. This paper proposes IBIS, a robust ensemble framework combining Inception-Bidirectional Long Short-Term Memory (BiLSTM) for feature extraction and Support Vector Machine (SVM) for classification of Doppler signatures. The proposed architecture specifically targets generalization capabilities. Experimental results on multiple datasets show that IBIS achieves 95.40% accuracy, delivering a 7.58% performance gain compared to standard architectures in cross-scenario evaluations on external datasets. The analysis confirms that IBIS effectively mitigates environmental dependency in Wi-Fi-based HAR.

**Index Terms**—IBIS, Channel State Information, Human Activity Recognition, Support Vector Machine, Inception, BiLSTM, Doppler traces, Ensemble Learning.

## I. INTRODUCTION

Wi-Fi sensing is an increasingly important technology that leverages ubiquitous Wi-Fi signals for non-intrusive Human Activity Recognition (HAR) [1]. Unlike traditional methods that rely on cameras or wearable sensors, Wi-Fi sensing utilizes Channel State Information (CSI) to capture and analyze subtle changes in signal propagation caused by human movement [2]. This approach is not only cost-effective but also preserves user privacy, making it highly suitable for applications in healthcare, surveillance, and smart homes.

However, a key challenge in this field is overfitting, where models trained on a specific dataset fail to generalize to new environments or unseen data. Many existing solutions, particularly those based on Convolutional Neural Networks (CNNs) [3] [4], are effective at capturing local patterns but often struggle to learn the broader, temporal dependencies

critical for robust generalization. Furthermore, raw CSI data frequently contains noise from hardware artifacts, such as phase and frequency oscillations, which can significantly hinder accurate movement interpretation and requires a rigorous sanitization process.

Recent studies have explored various approaches to enhance Wi-Fi sensing capabilities. Son et al. [5] improved indoor occupancy detection by proposing a pre-processing method that uses nonlinear transformations to expand CSI data into three channel vectors, which amplified signal differences. A CNN was then applied, achieving an average accuracy of approximately 95%. This work highlights the importance of effective signal pre-processing for boosting classification performance.

Ensemble learning has emerged as a key strategy to improve the reliability and accuracy of machine learning models. Wei et al. [6] used an ensemble learning approach for HAR by combining feature extraction with an SVM classifier.

Similarly, Ye et al. [7] developed a system for intrusion monitoring that combines Deep Neural Networks (DNNs) with BiLSTM networks. While their approach demonstrated improved performance over traditional methods, they noted a significant weakness in detecting specific actions, such as falling movements, with an accuracy of only 62.65%.

The SHARP algorithm, as proposed by Meneghello et al. [8], provides a foundational method for HAR based on Doppler traces. Their work addressed noise and hardware interference and, after applying a neural network-based refinement, achieved an accuracy of up to 95%. The authors also demonstrated that antenna merging could further enhance accuracy. Building upon this, Cominelli et al. [9] investigated the impact of Wi-Fi 6 features and developed a large-scale

A. M. Fernandes, H. I. Del Monego, B. S. Chang, and A. Munaretto are with the Universidade Tecnológica Federal do Paraná (UTFPR), Programa de Pós-Graduação em Engenharia Elétrica e Informática Industrial (CPGEI-CT), Av. Sete de Setembro, 3165, Curitiba, 80230-901, Brazil. Helder Fontes and Rui Campos are with INESC TEC, Faculdade de Engenharia, Universidade do Porto, Rua Dr. Roberto Frias, Porto, 4200-465, Porto, Portugal. Part of this work was submitted for presentation in Wireless Days 2025.

Corresponding author: Bruno S. Chang (e-mail: bschang@utfpr.edu.br).

This work was supported by the Coordination for the Improvement of Higher Education Personnel (CAPES) under ROR identifier: 00x0ma614 for the Article Processing Charge. This work was also supported by CNPq (444629/2024-6). This work was also partially supported by Instituto de Engenharia de Sistemas e Computadores, Pesquisa e Desenvolvimento do Brasil (INESC P&D Brasil). This research is part of the Instituto Nacional de Ciência e Tecnologia (INCT) of Intelligent Communications Networks and the Internet of Things (ICoNIoT), funded by CNPq (proc. 405940/2022-0) and CAPES (Finance Code 88887.954253/2024-00).

dataset for benchmarking. However, they reported difficulties in reproducing the SHARP algorithm's results, suggesting a sensitivity to environmental variability. Their findings also indicated that SHARP's performance degrades with decreased bandwidth and a higher number of activity classes.

Despite recent advances, Wi-Fi sensing still faces limited generalization to unseen data. Prior work, such as the CNN-ABLSTM cross-subject transfer learning method by He et al. [10], achieved 85.82% accuracy but highlighted the need for more robust models. Moreover, most existing studies rely only on the CSI amplitude, overlooking phase information, which is highly sensitive to noise and interference.

To address these gaps, we propose IBIS, a hybrid Inception-BiLSTM architecture combined with a non-linear SVM in the post-processing stage. Unlike conventional ensemble approaches that fuse models during training, IBIS leverages the probability outputs of internal neural layers as high-level feature vectors for the SVM, enabling sharper decision boundaries. Our framework operates solely on Doppler traces extracted from the CSI phase component, exploiting information typically ignored in the literature.

Expanding the introductory analysis presented in [11], IBIS was evaluated on five- and eight-class activity recognition tasks and compared against two state-of-the-art baselines: the SHARP algorithm [8] and an ABLSTM model using raw CSI [10]. To assess robustness across environments, we also included a complementary Doppler-based dataset [9]. The proposed method achieved an average accuracy of 95.40%, significantly outperforming all benchmark models and demonstrating strong generalization capabilities across different datasets and noise conditions.

The main contribution of this proposal is to improve the generalization capability of CSI data with respect to HAR by implementing a combination of spatial features and temporal sequences through the application of the proposed framework. This approach enables higher activity recognition accuracy. In addition, the inclusion of a SVM algorithm in the post-processing stage further enhances the framework, thereby demonstrating its effectiveness compared to traditional deep learning-based methods.

It is important to highlight that our proposal achieved better results compared to the related works presented in Table I. In terms of accuracy, the IBIS framework outperformed the works that use only amplitude. The main point is that when using phase information, it must be carefully handled to avoid possible classification errors caused by interference and existing offsets.

The remainder of this paper is organized as follows. Section II presents the definition of CSI as well as a detailed description of the datasets used in this study. Section III describes the development and implementation of the proposed algorithms, including the specific neural network architecture. The validation process, encompassing activity classification confusion matrices and Receiver Operating Characteristic (ROC) curve analysis, is presented in Section IV. Finally, Section V summarizes the main findings and provides concluding remarks.

## II. CHANNEL STATE INFORMATION DATA DESCRIPTION

This section presents the definition of CSI as adopted in IEEE 802.11 standard networks and also describes the datasets used in this proposal for data collection.

### A. Channel State Information

CSI is a data collection system that describes how a wireless signal propagates from the transmitter to the receiver. CSI captures the signal propagation characteristics in physical environments, including the combined effects of diffraction, reflection, and scattering [5].

Adopting the IEEE 802.11 standard, it employs advanced techniques such as Multiple-Input Multiple-Output (MIMO) and Orthogonal Frequency Division Multiplexing (OFDM) at the physical layer. These technologies aim to improve the supported data capacity and enhance channel orthogonality in environments affected by multipath propagation, which occurs when transmitted signals between the transmitter and receiver follow different paths due to phenomena like collisions and external interference.

For each transmitter/receiver antenna pair, CSI provides detailed information about the phase and amplitude attenuation experienced by the signal through multiple paths for each subcarrier. Specifically, the CSI for each subcarrier  $k$  between a transmitter with  $N_t$  antennas and a receiver with  $N_r$  antennas is represented by the matrix  $\mathbf{H}(k) \in \mathbb{C}$  [5]:

$$\mathbf{H}(k) = \begin{bmatrix} h_{11}(k) & \cdots & h_{1N_t}(k) \\ h_{21}(k) & \cdots & h_{2N_t}(k) \\ \vdots & \ddots & \vdots \\ h_{N_r1}(k) & \cdots & h_{N_rN_t}(k) \end{bmatrix}, k \in [1, K] \quad (1)$$

where  $K$  represents the number of subcarriers used, and  $h_{rc}(k)$  denotes the complex channel gain from the  $c$ -th transmitter antenna to the  $r$ -th receiver antenna. Each element  $h_{rc}(k)$  in the CSI matrix  $\mathbf{H}(k)$  can be decomposed into amplitude and phase components, as described by the following:

$$h_{rc}(k) = |h_{rc}(k)| \cdot \exp(j\theta_{rc}(k)), \quad (2)$$

where  $|h_{rc}(k)|$  is defined as the amplitude component, and  $\theta_{rc}(k)$  is the phase component of  $h_{rc}(k)$ .

Since CSI contains both amplitude and phase information for each subcarrier and for each pair of transmit and receive antennas, it provides high-resolution data compared to simple measurements such as RSS (Received Signal Strength). In this way, CSI data can be considered as a form of "imaging" of the signal propagation environment.

Changes in the environment, such as the presence or movement of people, directly affect Wi-Fi signal propagation. These alterations in the signal path also lead to variations in CSI. Since different people create distinct patterns, it is possible to estimate the number of individuals present by learning these patterns—this is the key concept behind people counting systems based on CSI-extracted data [5].

TABLE I  
SURVEY OF MODELS AND FEATURES IN USING CSI

Method / Authors	Year	Task	Model	Bandwidth	Network	Accuracy	CSI Data
Son et al. [5]	2024	Indoor Ocupancy	CNN	20 MHz	802.11	95%	Amplitude
WiAres [6]	2020	HAR	CNN+RF+SVM	-	802.11n	98.85%	Temporal / Spatial Correlation
SHARP [8]	2023	HAR	Inception	20/40/80 MHz	802.11	88.12%	Phase CFR
Cominelli et al. [9]	2023	HAR	Inception	20/40/80/160 MHz	802.11ac/ax	77.12%	Phase CFR
Ye et al. [7]	2024	HAR	DNN-ABLSTM	-	802.11n	92.06%	Amplitude and Phase
He et al. [10]	2025	HAR	CNN-ABLSTM	-	-	85.82%	Raw CSI
Widar [12]	2022	Gesture Recognition	CNN+RNN	-	-	92.7%	Amplitude
EfficientFi [13]	2022	HAR	CNN	40 MHz	802.11ax	98%	Amplitude
WiGr [14]	2022	Gesture Recognition	CNN+LSTM	40 MHz	802.11ax	86.8%–92.7%	Amplitude
Wi-SensiNet [15]	2024	HAR	CNN+BiLSTM	20 MHz	802.11	99%	Amplitude
IBIS*	2025	HAR	Inception-BiLSTM+SVM	80/160 MHz	802.11ac/ax	95.40%	Phase CFR

Note: The symbol \* represents our proposal Inception - BiLSTM + SVM architecture

## B. Dataset A

One of the datasets used for this research is based on the SHARP study [8] and consists of CSI data collected from three volunteers (one male, two females) performing eight activities in various indoor environments. These activities: empty, sitting, stand up, walking, running, jumping, and arm gym, were each recorded for 120 seconds. The data was gathered in a bedroom, living room, and university laboratory during two periods: April–December 2020 and January 2022. A Nexmon CSI Extraction Tool and an Asus RT-AC86U Wi-Fi router were used to extract the CSI from Wi-Fi 2.4 GHz preamble headers.

CSI is a data framework that describes how a wireless signal travels from a transmitter to a receiver. It provides high-resolution data on the physical propagation properties of a signal, including the effects of diffraction, reflection, and scattering [5]. Because CSI captures both amplitude and phase information, it is sensitive to environmental changes, such as the movement of people.

The dataset includes seven distinct scenarios (S1-S7):

- S1–S3: A bedroom with a central bookcase. S1 was used for model training, S2 for a generalization scenario, and S3 was measured on different days than S1;
- S4–S5: Activities performed alternately within the bedroom;
- S6: Data collected in a living room on different days;
- S7: A laboratory with numerous desks, computers, and monitors, measured over several days.

Scenario S7 was chosen as the benchmark for this study’s model evaluation because it presented the greatest challenge. According to the SHARP authors, the high density of obstacles and reflective surfaces in this environment significantly impacts CSI signal quality and classification performance.

## C. Dataset B

For application in the experiment, we considered using a second dataset, developed by Cominelli et al. [9]. Although originally designed for IEEE 802.11ax (Wi-Fi 6), thereby expanding the application scope. The main characteristics of this dataset are summarized below.

This dataset was developed using four Asus RT-AX86U routers interconnected to form a local-area network (LAN) and

controlled by a host notebook. One of the routers is configured to generate dummy Wi-Fi traffic at a constant rate through feature injection for AX-CSI, while the other three extract the corresponding CSI. According to the authors, due to the use of IEEE 802.11ax, data grows very rapidly, making it necessary to store the recordings in PCAP files.

Data collection was performed across seven different scenarios:

- S1 to S5: Conducted in the same physical environment, where neither the receivers nor the transmitter were moved during the entire duration of the experiments;
- S6: An office environment containing chairs and desks;
- S7: A large hall, representing an open environment without obstacles.

Twelve distinct activities were recorded: Walk, Run, Jump, Sitting, Empty room, Standing, Wave hands, Clapping, Lay down, Wiping, Squat, Stretching with a sampling rate of 80 samples per second.

For our experiment, scenario S2 was selected. This environment consists of a laboratory with reflective surfaces, which makes prediction more difficult.

Due to the accuracy challenges encountered with the original model, our intention is to apply the IBIS framework in different environments and scenarios in order to evaluate its behavior and robustness.

## III. SYSTEM MODELING

In this section, the main definitions related to the IBIS framework are presented, including the architectural composition, as well as the derived pseudocode outlining the main steps of the framework operation.

### A. Decision-Making Process and Algorithm Steps

To understand the purpose of our work, it is essential to first comprehend the SHARP method. After the CSI data is extracted from the Wi-Fi 802.11 ac/ax packet preambles, it undergoes three key stages, as shown in Figure 1:

1) *Pre-processing*: This stage sanitizes the CSI data by eliminating noise, interference, and phase ambiguity. A reference signal path is used to remove phase offsets, recovering a clean signal that reveals the Doppler traces associated with movement.

2) *Classification*: The sanitized Doppler traces are fed into an Inception neural network. To improve generalization beyond the original architecture's spatial feature learning capabilities, the network was enhanced with a BiLSTM layer, creating a hybrid Inception–BiLSTM model. This modification enables the architecture to capture both spatial and temporal dependencies, significantly boosting performance in human activity recognition. At this stage, it is possible to select the number of antennas used in the training process. The more antennas that are selected—up to the limit of four—the more distinctive information becomes available, consequently improving the neural network's recognition performance.

To understand how the IBIS operates, it is important to recognize the characteristics and advantages introduced by this new configuration. Unlike the original Inception network, additional layers are incorporated, providing enhanced data interpretation and improving the model's ability to extract discriminative features.

Figure 7 illustrates the integrated architecture of these two neural structures. While some layers like Normalization, Reshape, and Dropout are omitted for visualization, they are described in the text. Table II provides the input and output dimensions and parameter counts for each block. The shaded and hatched purple areas in the figure highlight the novel components of our proposal. Our approach enhances the standard Inception network, which typically only includes activation and convolution layers for learning local features. We added a MaxPooling layer and Batch Normalization to improve convergence and filter relevant features. Furthermore, a BiLSTM network was incorporated to enable the model to learn temporal patterns and motion dynamics from Doppler shifts.

**Inception Network:** This module is configured to extract spatial features from the Doppler trace data. A description of each block and its function is as follows:

- **Input:** The entry point for the Doppler trace data;
- **Normalization:** Normalizes input data by subtracting the mean and dividing by the standard deviation to stabilize training and improve convergence speed;
- **Conv2D (Conv Block):** This block combines Conv2D, Batch Normalization, and an Activation function. The Conv2D layer uses filters to extract local patterns like edges and textures;
- **Batch Normalization:** Normalizes activations to accelerate training and regularize the model;
- **Activation:** Introduces non-linearity, allowing the model to learn complex representations;
- **Max Pooling:** Reduces spatial resolution and complexity to focus on the most relevant features;
- **Concatenate:** Merges activation maps from different paths, maintaining important information while reducing dimensionality;
- **Dropout:** Randomly deactivates neurons during training to reduce overfitting and improve generalization;
- **Reshape:** Transforms the output tensor into a sequence format, preparing it for temporal processing by the BiLSTM layer.

The combination of Conv2D, Batch Normalization, and

Activation is repeated nine times within the Inception module, a core characteristic that increases depth and improves generalization by learning more abstract features.

**BiLSTM Network:** The second part of the architecture is the BiLSTM network, which was included to capture crucial temporal patterns and dependencies from the Doppler traces. These traces are time-series signals that reflect movement and channel variations, often exhibiting complex patterns that the network must recognize.

The BiLSTM network's components are described as follows:

- **BiLSTM + Attention:** This layer processes input sequences in both forward and backward directions, capturing complex temporal relationships. The attention mechanism enhances the model's focus on the most relevant time steps;
- **Global Average Pooling:** Reduces the dimensionality of the feature space in preparation for the final classification layer;
- **Dense Layer:** A fully connected layer that generates the final output, with the number of units depending on the number of output classes (Table II).

3) *Post-processing*: The original SHARP method used a majority voting mechanism among the four receiving antennas to determine the final activity label. This step smoothed outliers and improved robustness.

In this work, we modified the post-processing phase by introducing a Support Vector Machine (SVM) before the antenna fusion stage. This ensemble learning strategy leverages the SVM to enhance classification boundaries, thereby improving the overall precision and reliability of the final decision.

## B. Post-Processing Support Vector Machine

The hybrid Inception-BiLSTM neural network is effective at detecting and classifying both global patterns and temporal sequences. However, for accurate classification of CSI-derived data, this architecture alone is insufficient. To address this, an SVM was integrated into the post-processing stage as an ensemble learning strategy. Unlike common approaches where SVM is the primary classifier, this work uses it to refine the final classification results and improve generalization. The SVM's ability to handle outliers and its use of decision margins contribute to better model generalization, which is particularly useful for Doppler trace data that is prone to noise and distortions. This allows the SVM to refine the final classification results, especially for samples that might be misclassified by the neural network.

A key advantage of SVM lies in the flexibility of its kernel functions. The Radial Basis Function (RBF) kernel, as well as the Sigmoid and Polynomial kernels [16] [17] [18], are available options that can be selected for classification. In our framework, during the training stage, the SVM is trained using the probability outputs generated by the neural network. Through a grid-search optimization process, the most suitable kernel is determined for the underlying class distribution.

The penalty parameter C is also tuned to achieve an optimal balance between training accuracy and model generalization.

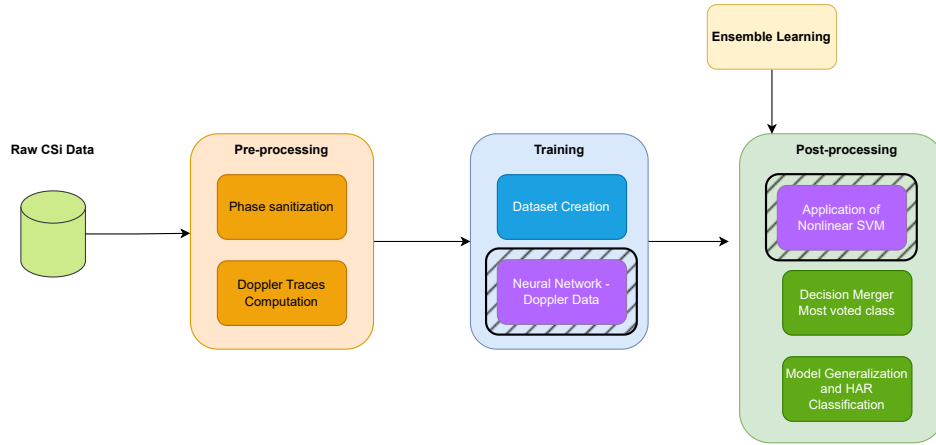


Fig. 1. The sequential process diagram illustrates the IBIS steps: collection of raw CSI data, passing through sanitization, neural network training, and Ensemble Learning post-Processing.

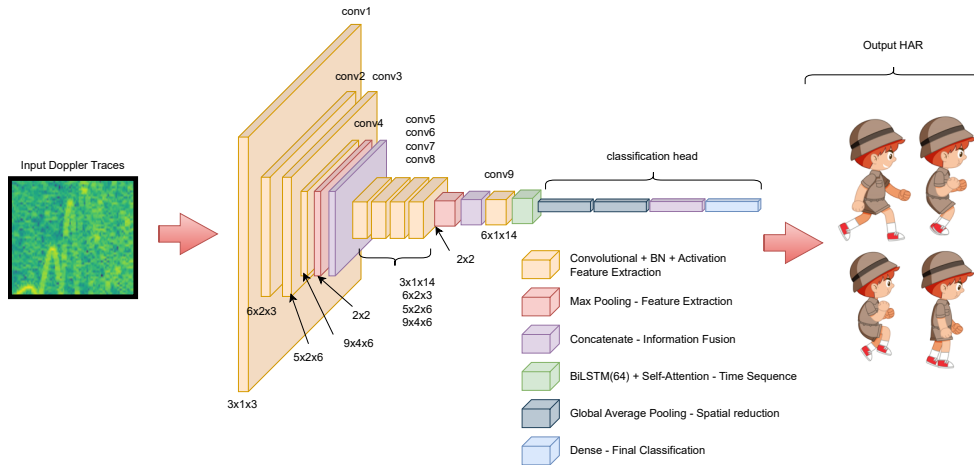


Fig. 2. Architecture of the Inception-BiLSTM hybrid neural network for Human Activity Recognition using Doppler traces, showing all convolutional and attention layers.

Furthermore, class balancing was applied to the SVM configuration to ensure that all classes receive equal weighting, preventing the classifier from becoming biased toward majority classes and resulting in a fairer and more robust overall prediction performance.

Figure 3 illustrates the SVM model's application, showing five distinct classes separated by well-defined boundaries. Proper class segmentation is essential for understanding the unique features of each class, leading to improved classification accuracy.

Regarding the hyperparameters, a learning rate of 0.001 was used for the hybrid network, along with an early stopping callback function to achieve the highest possible accuracy. At the classification stage, the SVM was also trained using a Grid Search, where three parameters were varied to determine the optimal training configuration. Initially, three kernel functions were considered: RBF, sigmoid, and polynomial, along with the trade-off parameter  $C$  and gamma ( $\gamma$ ), both ranging from 0.01 to 1, which are responsible for defining the decision

margins. The RBF kernel was ultimately selected by the Grid Search, representing the non-linear characteristics of the data.

The main reason for incorporating an SVM in the post-processing stage is that the Softmax layer of a neural network tends to force a probabilistic decision, even in highly ambiguous classes, and is sensitive to small variations in previously unseen environments. In contrast, the SVM aims to maximize the separation margin using high-level feature vectors, receiving a cleaner representation of class boundaries. This makes the inclusion of an SVM particularly suitable for noisy Doppler traces, where decision boundaries are not well defined. In this context, the combination of the BiLSTM module with dropout regularization, followed by the SVM in the post-processing step, contributes significantly to improving the model's generalization capability.

### C. Pseudocode

The pseudocode description presented in algorithm 1 concisely illustrates the application of the IBIS framework and

TABLE II  
INCEPTION-BILSTM ARCHITECTURE (COMPACT NOTATION)

Block / Layer	Output Shape	Parameters
Input Layer	(32, 32, 3)	-
Normalization	(32, 32, 3)	mean, variance
Conv2D(3×1×3)	(32, 32, 3)	3
BatchNormalization	(32, 32, 3)	12
Activation (swish)	(32, 32, 3)	-
Conv2D(6×2×3)	(31, 31, 6)	78
BatchNormalization	(31, 31, 6)	24
Activation (swish)	(31, 31, 6)	-
Conv2D(5×2×6)	(30, 30, 5)	125
BatchNormalization	(30, 30, 5)	20
Conv2D(9×4×6)	(28, 28, 9)	873
BatchNormalization	(28, 28, 9)	36
Activation (swish)	(30×30×5) / (28×28×9)	-
MaxPooling2D(2×2)	(15, 15, 5)	-
Concatenate	(15, 15, 14)	-
Conv2D(3×1×14)	(15, 15, 3)	45
BatchNormalization	(15, 15, 3)	12
Activation (swish)	(15, 15, 3)	-
Conv2D(6×2×3)	(14, 14, 6)	78
BatchNormalization	(14, 14, 6)	24
Conv2D(5×2×6)	(13, 13, 5)	125
BatchNormalization	(13, 13, 5)	20
Conv2D(9×4×6)	(11, 11, 9)	873
BatchNormalization	(11, 11, 9)	36
Activation (swish)	(13×13×5) / (11×11×9)	-
MaxPooling2D(2×2)	(6, 6, 5)	-
Concatenate	(6, 6, 14)	-
Dropout(0.5)	(6, 6, 14)	-
Conv2D(6×1×14)	(6, 6, 6)	84
BatchNormalization	(6, 6, 6)	24
Activation (swish)	(6, 6, 6)	-
Reshape	(36, 6)	-
Bidirectional LSTM (64 units)	(36, 128)	45568
Activation (tanh)	(36, 128)	-
Attention	(36, 128)	16640
GlobalAvgPooling1D (RNN)	(128,)	-
GlobalAvgPooling1D (Attention)	(128,)	-
Concatenate	(256,)	-
Dropout(0.5)	(256,)	-
Dense (5 classes)	(5,)	1285

Note: ‘Conv2D(out×kernel×in)’ notation refers to output channels, filter size (square or rectangular kernel), and input channels, respectively. Shapes may vary slightly depending on padding/stride.

the main processes involved.

It is worth mentioning that the code containing the modifications to the SHARP algorithm, as well as all stages of the IBIS implementation, will be made public after the publication of this proposal.

#### IV. PERFORMANCE EVALUATION

This section evaluates the IBIS framework using generalization data from Scenario S7 for Dataset A and from Scenario S2 for Dataset B, as previously described. It is important to note that this validation used an 80 MHz bandwidth (IEEE 802.11ac) for Scenario S7 and a 160 MHz bandwidth (IEEE 802.11ax) for Scenario S2, with the selection of four antennas to maximize the amount of information obtained during training. This scenario, a laboratory room filled with desks, chairs, and monitors, was chosen as a benchmark due to its challenging nature. The numerous obstacles in

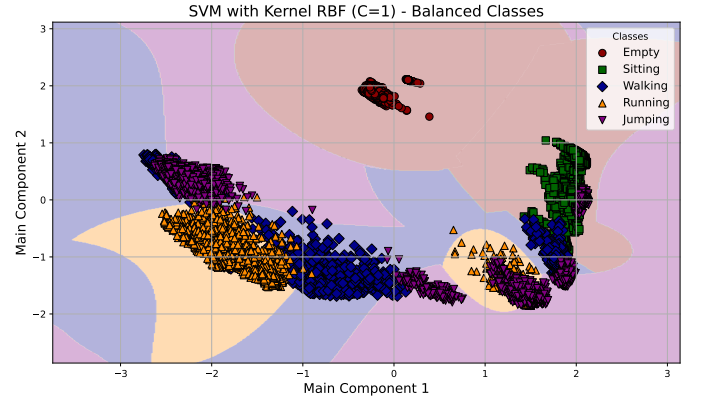


Fig. 3. Representation of the SVM algorithm applied to five movements with non-linear Data, applying the PCA method for dimensionality reduction.

this setup introduce complex signal distortions like multipath propagation, reflection, and scattering, which make the task of activity recognition particularly difficult for any classifier. We will analyze the model’s performance through its learning curves, class-wise confusion matrices, and the computational cost of the hybrid architecture.

For data separation, after Doppler extraction, the dataset was divided into 60%, 20%, and 20% for training, testing, and validation, respectively.

To avoid decision bias in the evaluated algorithms, ten simulations were performed for each experiment, and the results provided herein represent the average across the ten simulations.

#### A. Confusion Matrix for 5 Movements

Figure 4 compares the confusion matrices for five movements, showing the results from the Inception-only network against the proposed hybrid scheme. As seen in Figure 4a, the Inception network struggled with precision, particularly for the walking movement, which was frequently confused with running, achieving only 71% accuracy. Jumping was also often misclassified as running, with an accuracy of just 70%. This lack of precision is attributed to the similarity of Doppler patterns between these movements and the fact that the Inception network was not designed to handle temporal dependencies crucial for accurate CSI data classification.

Conversely, Figure 4b shows the results obtained after implementing our IBIS framework, which achieved substantially better performance with only minor misclassifications. A more balanced distribution of accuracy across the classes is also observed, reaching up to 99% in categories where the original model previously exhibited confusion. Overall, this configuration yields a 7.58% performance gain compared to the previous simulation.

This improvement is primarily attributed to the BiLSTM component’s ability to capture temporal patterns from the Doppler data. In addition, the SVM—through the selection of an appropriate kernel, proper tuning of the parameter  $C$ , and class balancing—further refined the classification boundaries,

**Algorithm 1** IBIS framework

- 1: **Preprocessing:**
- 2:   Apply LASSO-based sanitization and remove offset
- 3:   Extract Doppler traces and select subcarriers
- 4: **Input:** Dataset  $X$ , labels  $Y$ , batch size 32, learning rate 0.001, epochs 100
- 5:   Normalize features:  $X_{\text{norm}} = \text{normalize}(X)$
- 6:   Split dataset:  $(X_{\text{train}}, Y_{\text{train}}, X_{\text{test}}, Y_{\text{test}}) \leftarrow \text{split}(X_{\text{norm}}, Y, 0.8)$
- 7: **Inception Feature Extraction:**
- 8:   Apply parallel convolutions with multiple kernel sizes
- 9:   Concatenate outputs to obtain  $F_{\text{inception}}$
- 10: **BiLSTM Temporal Modeling:**
- 11:   Feed  $F_{\text{inception}}$  into BiLSTM layers
- 12:   Extract temporal representation  $F_{\text{BiLSTM}}$
- 13: **Softmax Classification:**
- 14:   Compute posterior probabilities:
- 15:      $P(Y|X) = \text{Softmax}(W_s F_{\text{BiLSTM}} + b_s)$
- 16:   Perform Grid Search to select kernel type,  $C$ , and  $\gamma$
- 17: **SVM Training (Postprocessing):**
- 18:   Train SVM using  $(P(Y|X_{\text{train}}), Y_{\text{train}})$
- 19:   Available kernels:
- 20:     **RBF:**  $K(x, x') = \exp(-\gamma \|x - x'\|^2)$
- 21:     **Sigmoid:**  $K(x, x') = \tanh(\gamma x^\top x' + r)$
- 22:     **Polynomial:**  $K(x, x') = (\gamma x^\top x' + r)^d$
- 23: **Prediction:**
- 24:   Compute  $P(Y|X_{\text{test}})$  using the Inception–BiLSTM–Softmax network
- 25:   Predict:  $Y_{\text{pred}} = \text{SVM.predict}(P(Y|X_{\text{test}}))$
- 26: **Evaluation:**
- 27:   Compute Accuracy, Precision, Recall, and F1-score
- 28: **Output:** Final predictions  $Y_{\text{pred}}$  and evaluation metrics

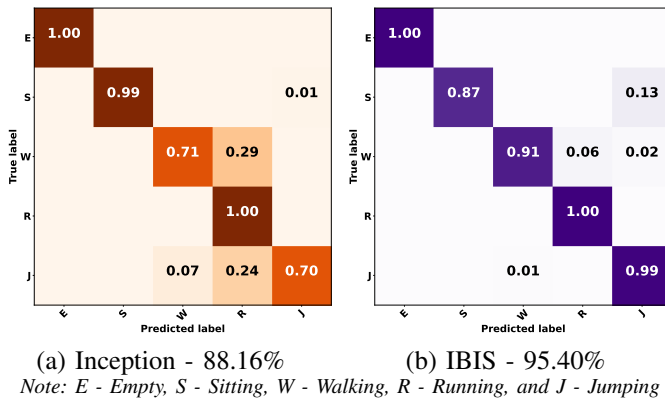


Fig. 4. Comparative analysis of the confusion matrix for five movements: original Inception versus IBIS

resulting in enhanced overall performance. Both confusion matrices shown correspond to the post-antenna fusion stage, where classification decisions are merged using majority voting.

### B. ROC Curve for 5 Movements

Figure 5 displays the learning ROC curve for all five classes, with a dotted diagonal line indicating the classification

threshold. This curve was generated using generalization test data without antenna fusion, allowing for a direct evaluation of the algorithm’s generalization capability.

As shown in Figure 5a, the original model performed poorly for the walking, running, and jumping classes, which exhibited significant fluctuations in accuracy. In contrast, Figure 5b shows that, with our proposed approach, the accuracy values increased and became more stable, with no apparent oscillations, even without antenna fusion, except for the Walking class. At this stage, we are evaluating only the effect of applying the SVM after training the neural network using the softmax probabilities as input. In other words, this result reflects exclusively the effectiveness of the SVM refinement, excluding the majority-voting step from antenna fusion, which is applied afterward. However, when considering the class distribution, the results are more uniform. This highlights the effectiveness of incorporating ensemble learning in this challenging scenario.

### C. Confusion Matrix for 8 Movements

Figure 6 shows the confusion matrices for eight movements, including standing, stand up, and arm gym. In Figure 6a, the performance of the original algorithm deteriorated compared to the five-movement scenario, exhibiting a higher misclassification rate for gestures such as arm gym, jumping, and sitting, resulting in an accuracy of 38.38%. This is likely due to the SHARP algorithm’s sanitization process, where the error probability increases proportionally to the number of classified gestures and bandwidth [9]. This behavior indicates that the original model struggled with overfitting and failed to generalize when more movements were added. In contrast, Figure 6b shows that the overall accuracy remained high despite the addition of new movements, reaching 70.25%. This superior performance is attributed to the combination of the Inception–BiLSTM hybrid network and the SVM algorithm. Even after attempting to improve the original model’s performance by modifying the dataset split to 80% for training, 10% for testing, and 10% for validation, the results remained unchanged.

### D. Doppler Traces

In Figure 7, we present the Doppler trace plots for eight activities. It is possible to observe that the traces corresponding to the Empty, Sitting, Standing, and Arm Gym activities exhibit very similar movement patterns, making them difficult for a neural network to distinguish. Consequently, their spatial features lie very close to one another. In this context, the BiLSTM network combined with the SVM becomes the decisive component: the BiLSTM is able to extract temporal dependencies, and once these dependencies are captured, the SVM refines the decision boundaries through appropriate tuning of the trade-off parameter, kernel choice, and margin.

It becomes clear that, even with IBIS, the framework struggles to reliably distinguish highly similar Doppler traces due to the strong overlap between activities. This reinforces the need for a carefully designed preprocessing pipeline. Moreover, depending on the normalization strategy, relevant

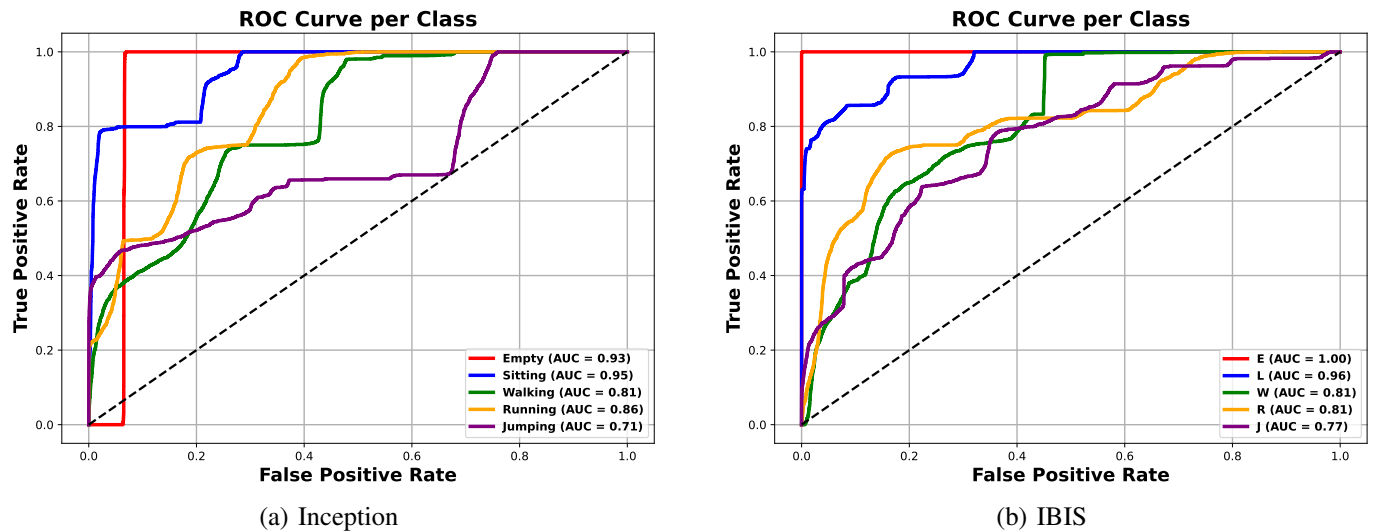


Fig. 5. ROC curve analysis for five movements: comparing the original Inception with IBIS

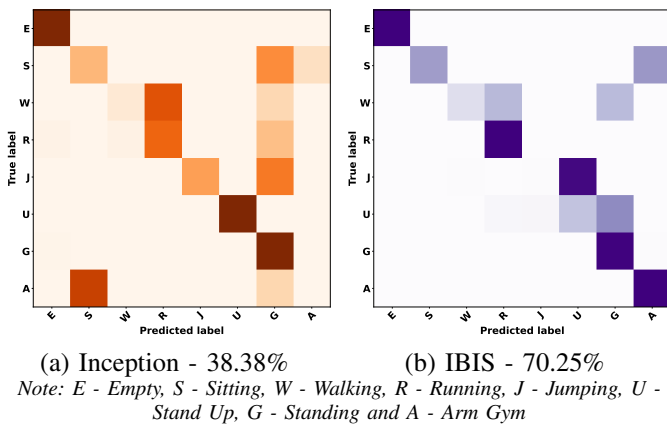


Fig. 6. Comparative analysis of the confusion matrix for eight movements: original Inception versus IBIS

offsets and peak-related features may be suppressed, which are essential for accurate neural network inference. Nevertheless, IBIS still outperforms the original Inception network, yielding an improvement of approximately 45.30%.

### E. Ablation

The next experiment conducted with our framework aims to evaluate its behavior when individual components of the pipeline are removed. First, we run the experiment using the SVM together with the Inception network and the full IBIS model. In the second step, we remove the SVM from the composition, leaving only the Inception–BiLSTM neural network. Analyzing the first experiment in Figure 8, we observe that the Inception model with SVM experiences a reduction in performance, achieving 85.27%, whereas the full IBIS model reaches 95.40%.

Removing the SVM from the pipeline resulted in a 2% increase in accuracy, highlighting the contribution of the BiLSTM component, which achieved 90% compared to the 88% produced by the original Inception network. When this performance is compared with the 95.40% obtained by the

complete framework, it becomes clear that the SVM plays a predominant role, as most of the accuracy gain originates from its inclusion in the post-processing stage, where it effectively refines class boundaries with high precision.

Another experiment involved removing the Doppler traces from the pipeline and applying IBIS directly to the sanitized data. Analyzing Figure 8, on the right-hand side, we observe that the Inception network without Doppler information reaches 34% accuracy, while IBIS achieves 49%. Although both results are lower, this confirms that Doppler features play a fundamental role in the analysis of phase components. For this specific dataset, removing Doppler information leads to a substantial degradation in accuracy, especially for the Inception network.

### F. Exploring another dataset

With the intention of demonstrating the efficiency of the IBIS framework, new experiments were conducted using the public dataset provided by Cominelli et al. [9]. In this experiment, Scenario S2 was used, and—similarly to the previous experiments—the Grid Search technique was applied to select the trade-off parameter  $C$  and the  $\gamma$  parameter, as well as to evaluate different kernels, including RBF, Sigmoid, and Polynomial. Thus, the exact same procedure adopted in our framework was applied here, but now with a different dataset.

In this previously described dataset, several SHARP adaptations were applied to support operation with a 160 MHz bandwidth. Five activities—Walking, Running, Jumping, Sitting, and Empty Room, were evaluated, as shown in the confusion matrix presented in Figure 9. Based on this dataset, adjustments were also made to the scripts to make them more consistent with those used in the other dataset.

It is important to highlight that, unlike the previous dataset, the IBIS framework was not able to effectively distinguish between the walking and running activities in this dataset. This limitation is mainly due to the reduced amount of available information: after generating the Doppler traces, the window segments created during the dataset splitting and training

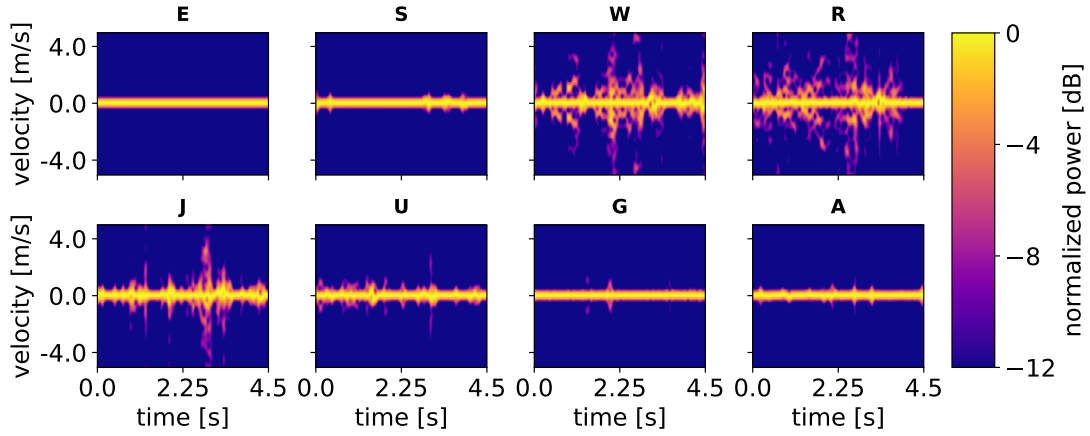


Fig. 7. Doppler traces for the activities: E – Empty, S – Sitting, W – Walking, R – Running, J – Jumping, U – Stand Up, G – Standing, A – Arm Gym.

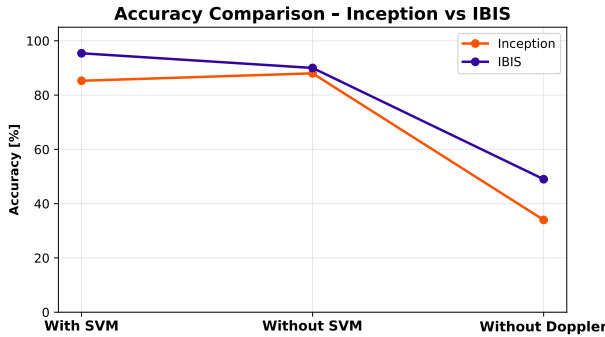


Fig. 8. Graph illustrating the behavior of the accuracy when removing the Doppler traces and/or the SVM components

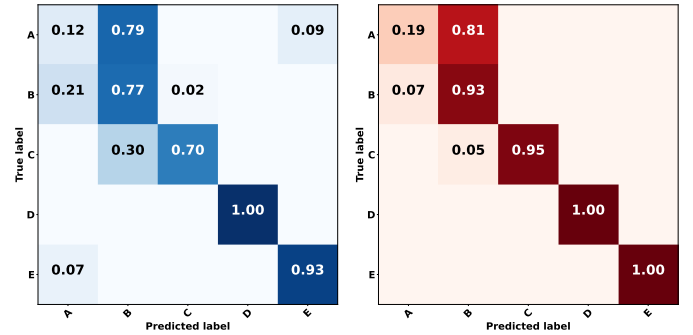
stages become significantly smaller. As a result, the IBIS does not receive sufficient information to reliably differentiate between these two activities.

Analyzing Figure 9, we observe that the Inception network alone achieved an accuracy of 70.23%, whereas the IBIS framework reached 81.40%, representing an accuracy gain of 13.72%. This difference in performance between datasets can be attributed to variations in data distribution; elements such as obstacles, walls, and interference introduce additional complexity and reduce recognition performance due to the increased similarity between activity patterns.

These experiments demonstrate that IBIS maintains superior performance across different datasets, achieving substantial improvements even under varying environmental conditions and inherent limitations.

### G. Comparable Algorithms

Table III demonstrates that the IBIS framework achieved the best and most consistent results compared to other ensemble learning models. Its superior performance is attributed to the neural network's ability to capture complex patterns and the SVM's capacity to handle temporal sequence boundaries, both of which are essential for Doppler-based data. The original



(a) Inception - 70.23%

(b) IBIS - 81.40%

Note: A - Walking, B - Run, C - Jump, D - Sitting, and E - Empty Room

Fig. 9. Comparative analysis of the confusion matrices for five activities: original Inception model versus the IBIS, using the dataset from Cominelli et al. [9]

Inception model, for example, struggled with classifying similar movements like walking and jumping, leading to false positives and poor generalization.

TABLE III  
MODELS ACCURACY

Models	Empty(%)	Sitting(%)	Walking(%)	Running(%)	Jumping(%)
IBIS	100	87	91	100	99
Inception	100	99	71	100	70

Similarly, Table IV, which presents average metrics for five movement classes, confirms that our IBIS outperformed other tested models. We included additional metrics like F1-score, recall, and precision to provide a more comprehensive evaluation, as relying solely on accuracy can be misleading. These metrics help assess the model's performance in imbalanced scenarios and its ability to balance precision and recall.

While the CNN-ABLSTM model from a related study [10] presents a lower computational cost due to its lighter architecture, it achieves only 85.82% accuracy, whereas our IBIS method reaches 95.40%. This 10.04% improvement under the

TABLE IV  
AVERAGE MODELS METRICS FOR 5 MOVEMENTS

Models	Accuracy(%)	F1 Score(%)	Recall(%)	Precision(%)
<b>IBIS</b>	<b>95.40</b>	<b>95.21</b>	<b>95.30</b>	<b>95.57</b>
Inception	88.16	88.26	87.87	91.47

same 100-epoch training condition is primarily due to the limited number of attention layers and the reduced architectural complexity in their model, which hinder its ability to capture complex temporal-spatial patterns and subtle Doppler-induced variations. In contrast, our IBIS framework leverages the Inception module for spatial feature extraction and the BiLSTM module for temporal dependency learning, making it more robust to noise, interference, and reflective-surface effects. Additionally, our pipeline integrates advanced signal processing, the SHARP algorithm for noise suppression, and traditional machine learning SVM for refined classification. This combined approach significantly improves generalization compared to the transfer-learning-based model trained on raw, unprocessed data in [10].

#### H. Computational Complexity

A primary challenge with neural networks is computational cost, as a deeper network with more layers typically consumes more resources. To objectively measure this, Figure 10 shows the computational cost over 100 training epochs without using callbacks like early stopping.

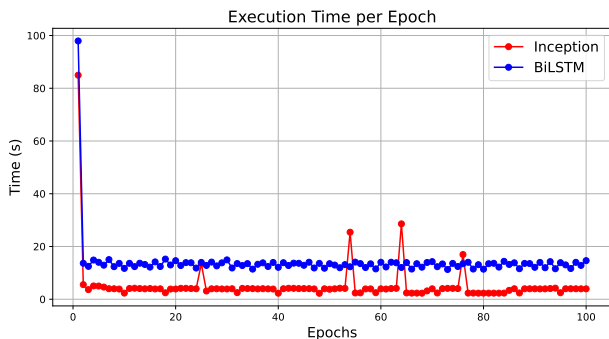


Fig. 10. Graph illustrating the execution time per training epoch for both the original Inception architecture and the proposed hybrid IBIS model.

We evaluated two distinct architectures:

- The original Inception network;
- An Inception network combined with a BiLSTM layer.

The standalone Inception network had the lowest computational cost and the shortest training time per epoch due to its shallow architecture. However, it failed to accurately classify movements, producing false positives and showing temporal instability. It should be noted that the SVM classifier is not displayed in this figure because it is not involved in the epoch-level training process. The SVM is fitted only once after the neural network has converged, using the extracted feature probabilities. Consequently, its computational overhead

is negligible, and its inclusion in the graphical representation is unnecessary.

## V. CONCLUSION

This paper addresses the challenges of generalization and robustness in HAR using non-intrusive Wi-Fi sensing. We propose IBIS, a novel hybrid architecture that strategically integrates Inception layers for spatial feature extraction, a BiLSTM module for temporal modeling, and an SVM classifier for sharper decision boundaries. Extensive evaluations across scenarios with different activity sets (five and eight classes) demonstrate the framework's effectiveness, reaching an average accuracy of 95.40%. Notably, IBIS outperforms the state-of-the-art SHARP method by 7.58% on Dataset A, highlighting its superior capability in handling noise and environmental interference. A second improvement of 13.40% was observed on Dataset B, largely due to environmental differences, where variations in surface materials and layout can alter signal propagation patterns. Nevertheless, even under new conditions and datasets, IBIS consistently delivers superior performance. The analysis further confirms that replacing the standard Softmax layer with an SVM classifier significantly enhances classification performance in complex environments. Future work will focus on optimizing the Doppler trace acquisition and pre-processing stages to reduce computational complexity and further streamline the training pipeline.

## REFERENCES

- [1] I. Ahmad, A. Ullah, and W. Choi, "Wifi-based human sensing with deep learning: Recent advances, challenges, and opportunities," *IEEE Open Journal of the Communications Society*, vol. 5, pp. 3595–3623, 2024.
- [2] J. Yang, X. Chen, H. Zou, D. Wang, Q. Xu, and L. Xie, "Efficientfi: Toward large-scale lightweight wifi sensing via csi compression," *IEEE Internet of Things Journal*, vol. 9, no. 15, pp. 13 086–13 095, 2022.
- [3] X. Chen, Y. Zou, C. Li, and W. Xiao, "A deep learning based lightweight human activity recognition system using reconstructed wifi csi," *IEEE Transactions on Human-Machine Systems*, vol. 54, no. 1, pp. 68–78, 2024.
- [4] D. Khan and I. W.-H. Ho, "Deep learning of csi for efficient device-free human activity recognition," in *2021 IEEE 7th World Forum on Internet of Things (WF-IoT)*, 2021, pp. 19–24.
- [5] J. Son and J. Park, "Channel state information (csi) amplitude coloring scheme for enhancing accuracy of an indoor occupancy detection system using wi-fi sensing," *Applied Sciences*, vol. 14, no. 17, 2024. [Online]. Available: <https://www.mdpi.com/2076-3417/14/17/7850>
- [6] W. Cui, B. Li, L. Zhang, and Z. Chen, "Device-free single-user activity recognition using diversified deep ensemble learning," *Applied Soft Computing*, vol. 102, p. 107066, 2021.
- [7] C. Ye, S. Xu, Z. He, Y. Yin, T. Ohtsuki, and G. Gui, "Non-contact cross-person activity recognition by deep metric ensemble learning," *Bioengineering*, vol. 11, no. 11, 2024.
- [8] F. Meneghello, D. Garlisi, N. D. Fabbro, I. Tinnirello, and M. Rossi, "Sharp: Environment and person independent activity recognition with commodity ieee 802.11 access points," *IEEE Transactions on Mobile Computing*, vol. 22, no. 10, pp. 6160–6175, 2023.
- [9] M. Cominelli, F. Gringoli, and F. Restuccia, "Exposing the CSI: A Systematic Investigation of CSI-based Wi-Fi Sensing Capabilities and Limitations," in *2023 IEEE International Conference on Pervasive Computing and Communications (PerCom)*, 2023, pp. 81–90.
- [10] Z. He, M. Bouazizi, G. Gui, and T. Ohtsuki, "A cross-subject transfer learning method for csi-based wireless sensing," *IEEE Internet of Things Journal*, vol. 12, no. 13, pp. 23 946–23 960, 2025.
- [11] A. Fernandes, H. Monego, B. Chang, A. Munaretto, H. Fontes, and R. Campos, "Hybrid inception-bilstm and svm for enhanced csi-based human activity recognition," 12 2025, pp. 1–5.

- [12] Y. Zhang, Y. Zheng, K. Qian, G. Zhang, Y. Liu, C. Wu, and Z. Yang, "Widar3.0: Zero-effort cross-domain gesture recognition with wi-fi," *IEEE Transactions on Pattern Analysis and Machine Intelligence*, vol. 44, no. 11, pp. 8671–8688, 2022.
- [13] J. Yang, X. Chen, H. Zou, D. Wang, Q. Xu, and L. Xie, "Efficientfi: Toward large-scale lightweight wifi sensing via csi compression," *IEEE Internet of Things Journal*, vol. 9, no. 15, pp. 13 086–13 095, 2022.
- [14] X. Zhang, C. Tang, K. Yin, and Q. Ni, "Wifi-based cross-domain gesture recognition via modified prototypical networks," *IEEE Internet of Things Journal*, vol. 9, no. 11, pp. 8584–8596, 2022.
- [15] X. Fu, C. Wang, and S. Li, "Wi-sensinet: Through-wall human activity recognition based on wifi sensing," in *2024 5th International Conference on Big Data & Artificial Intelligence & Software Engineering (ICBASE)*, 2024, pp. 238–241.
- [16] K. Kolodiazhnyi, *Hands-On Machine Learning with C++*. Packt Publishing, 2020, accessed: 2025-05-17. [Online]. Available: <https://www.packtpub.com/product/hands-on-machine-learning-with-c/9781800203257>
- [17] Z. Ye and H. Li, "Based on radial basis kernel function of support vector machines for speaker recognition," in *2012 5th International Congress on Image and Signal Processing*, 2012, pp. 1584–1587.
- [18] A. Patle and D. S. Chouhan, "Svm kernel functions for classification," in *2013 International Conference on Advances in Technology and Engineering (ICATE)*, 2013, pp. 1–9.



**ALISON M. FERNANDES** received a B.Sc. degree in Electrical Engineering from the Federal University of Technology – Paraná (UTFPR) in 2016. In 2021, he completed a second B.Sc. degree in Electronic Engineering at the same university. In 2025, he received his M.Sc. degree. He is currently pursuing a Ph.D. in Electrical Engineering and Industrial Informatics at UTFPR. During his undergraduate studies, he conducted research in power systems, electronics, and embedded systems. His main areas of

interest include programming, intelligent networks, machine learning, artificial neural networks, and generative artificial intelligence (AI) networks.



**HERMES I. DEL MONEGO** received the B.Sc. Degree in Computer Science from Positivo University Brazil in 2000, an M.Sc. degree from the Federal University of Technology - Paraná (UTFPR), and a Ph.D. in Electrical Engineering and Computing from the Faculty of Engineering of Porto University (FEUP) in 2011. Since 2010, he has been with the Electronics Department at the Federal University of Technology – Paraná (UTFPR), where he is now an associate professor. He has been invited to conduct research

at INESC TEC, Porto, Portugal, and is the academic director at INESC P&D Brazil. His main research topics include computer networks, cellular networks, radio resource management, traffic distribution, and handover management.



**BRUNO S. CHANG** was born in Curitiba, Paraná, Brazil, in 1984. He received the B.Sc. Degree in Telecommunications Engineering from the Regional University of Blumenau (FURB), Brazil, in 2006, the M.Sc. degree in electrical engineering from the Federal University of Santa Catarina (UFSC), Florianópolis, Brazil, in 2008, and the D.Sc. degree in electrical engineering from the Federal University of Santa Catarina (UFSC), Florianópolis, Brazil, and the Conservatoire National des Arts et Métiers (CNAM), Paris, France in 2012. He was a visiting professor at CNAM in 2018 and a visiting researcher at INESC TEC Porto, Portugal in 2024. He is currently an Associate Professor at the Federal University of Technology - Paraná (UTFPR), Curitiba, Brazil. His main research interests lie in the areas of digital communications and signal processing, including multi-carrier systems, detection and estimation algorithms, widely linear processing and energy efficient communications.



**ANELISE MUNARETTO** received the Dipl.Ing. Degree in Computer Engineering from the Pontifical Catholic University of Parana, Brazil, in 1994, and the M.S. and Ph.D. degrees in Computer Science from Université Pierre et Marie Curie (UPMC–Sorbonne Universités), in 2001 and 2004, respectively. Since 2005, she has been with the Federal University of Technology–Paraná (UTFPR), where she is currently a Full Professor. Her research interests include computer networks with an emphasis on do-

mains related to mobile networking, the Internet of Things (IoT), and smart cities.



**RUI CAMPOS** received the Ph.D. degree in electrical and computer engineering from the University of Porto, in 2011. He is currently a Senior Researcher and a Coordinator of the Centre for Telecommunications and Multimedia, INESC TEC, and an Assistant Professor with the University of Porto, where he teaches courses on telecommunications. He has coordinated several research projects, including the WiFIX project in CONFINE Open Call 1, SIMBED (Fed4FIRE+OC3), and SIMBED+ (Fed4FIRE+OC5). He has also participated in several EU research projects, including H2020 ResponDrone, H2020 RAWFIE, FP7 SUNNY, and FP6 Ambient Networks. He is the author of more than 85 scientific publications in international conferences and journals with peer review. His research interests include airborne, maritime, and green networks, with a special focus on medium access control, radio resource management, and network auto configuration. He has been a TPC Member of several international conferences, including IEEE INFOCOM, IEEE ISCC, and IFIP/IEEE Wireless Days. He was the General Chair of Wireless Days 2017 and the TPC Vice-Chair of 2021 Joint EuCNC and 6G. Summit.



**HELDER FONTES** received the M.Sc. degree in 2010 and the Ph.D. degree in 2019, in informatics engineering from the Faculty of Engineering, University of Porto, Portugal. He has been an advisor of more than 10 M.Sc. theses on wireless networking simulation, emulation, and experimentation. He is currently the Coordinator of the Wireless Networks (WiN) area with INESC TEC, and since 2009, he has been participating in multiple national and EU research projects, including SITMe, HiperWire-

less, FP7 SUNNY, H2020 ResponDrone, DECARBONIZE, FLY.PT and Fed4FIRE+ SIMBED, and SIMBED+ and SMART open call projects. His research interests include wireless networking simulation, emulation, and experimentation in the scope of emerging scenarios such as airborne and maritime, with a special focus on repeatability and reproducibility of experiments using digital twins of wireless testbeds.